AR-002-541

DEPARTMENT OF DEFENCE

DEFENCE SCIENCE AND TECHNOLOGY ORGANISATION

ELECTRONICS RESEARCH LABORATORY

TECHNICAL REPORT

ERL-0181-TR

IONOSPHERIC TRANSEQUATORIAL RADIO WAVE GUIDANCE AT VHF

C. Winkler

S U M M A R Y

The mechanism of reflection of radio waves at VHF from irregularities aligned with the earth's magnetic field in the equatorial region is examined in detail and a computer-based study of the resulting phenomenon is presented.

POSTAL ADDRESS: Chief Superintendent, Electronics Research Laboratory, Box 2151, GPO, Adelaide, South Australia, 5001.

TABLE OF CONTENTS

LIST OF APPENDICES

LIST OF FIGURES

1. INTRODUCTION

There has been a continuing interest in the use of the VHF band to provide communication channels which supplement those of the more conventional but congested HF band. The availability of these supplementary channels for large range transequatorial circuits was first reported by radio amateurs and studies of the phenomenon were largely experimental. The physical mechanisms involved in producing these channels have been and still are poorly understood. It is the purpose of this report to lay down the elements of a simple theory to explain the large signal strengths observed on these circuits and to describe the results of a computer model used to calculate them.

A qualitative review of a variety of proposed mechanisms involved in producing these long distance circuits appeared in 1969(ref.1). This review also contains an excellent historical background and we will not attempt to repeat that here. There were essentially four possible ways in which these circuits could be set up.

(1) Refraction in an undisturbed F region plasma. The occurrence of bulges in the ionization densities on each side of the equator is assumed to provide sufficient gradation in the refractive index to allow this to take place.

(2) Guidance by steep field aligned gradients in electron density. The ray path is assumed to be given a curvature equal to the field curvature so that guidance occurs along steeply varying gradients of ionization.

(3) Scatter from F region irregularities. An ensemble of scatterers at ionospheric height cannot return sufficient power to the opposite hemisphere unless it is shaped to provide a degree of coherence that is deemed to be unlikely.

(4) Double scattering between irregularities. Scattering from irregularities on one side of the equator to a similar set in the opposite hemisphere provides the correct geometry but considerable debate exists over the magnitude of the received power.

None of these mechanisms was entirely adequate to explain the phenomena of transequatorial propagation (TEP) and since the study was of a semi-empirical nature no firm conclusions could be reached. An attempt has since been carried out to determine the physical extent of field guided F region irregularities at the equatorial peak by illuminating them with a sideways looking VHF radar(ref.2) but the nature of the irregularities remained obscure.

More recently large scale regions of depleted ionospheric plasma, called bubbles, have been discovered and observed from the ground(ref.3) and from satellite (ref.4). A description of TEP of radio waves at VHF has also appeared attributing it to guidance(ref.5) along field aligned tubes of depleted ionization resulting from the post sunset creation of equatorial plasma bubbles. A large ensemble of these bubbles were then imagined to contribute the observed characteristics but some unusual and dubious properties were ascribed to the waveguide tubes.

In this report we consider the properties of a curved idealized dielectric discontinuity formed at the upper edge of a rising plasma bubble. The equations for reflection and guidance of electromagnetic waves along the discontinuity are programmed onto a high speed digital computer and profiles for the received power at points on the surface of the earth in the receiving hemisphere are derived. A comparison with some experimental results for a Darwin to Yamagawa circuit is also included.

2. THE MODELS

The situation is illustrated in figure 1 which shows a transmitter at point A in one hemisphere and a receiver at point B in the opposite hemisphere. The geographic equator is located at G and the geomagnetic equator is at position M. The magnetic field structure is assumed to be identical with that of a magnetic dipole located at the centre of the earth so that field lines are symmetrical about the geomagnetic equator.

In the situation we have here a dielectric discontinuity is assumed to be exactly aligned with the particular field line coincident with the top edge of a rising plasma bubble. The plasma bubble represents a region of depleted ionization (refs.3,4,6) for which we take the refractive index as being identically one. Where the ionization is not totally depleted then the refractive index is only close to one but detailed studies of this marginal effect are left to a later report.

Since the complete modal solution for this problem is extremely difficult, if not impossible, then it is necessary to resort to simplified methods. One method that we can use in this situation is based on some simple concepts from geometric optics. We discuss the ray approximations in some detail in the following sections.

2.1 The Ionospheric Models

It is shown in Appendix I that the field lines near the equator assume a shape very close to elliptical (within 1%). Furthermore it has also been shown that elliptical multimode dielectric waveguiding structures(refs.7,8) can be well represented using an extended form of geometric optics which allows for tunnelling from curved dielectric surfaces.

An appropriate model for the ionospheric electron density is the Chapman model described in Appendix II. The change in electron density is related to a change in refractive index as given in Appendix III. Combing these two results one can readily see that the refractive index discontinuity varies with height above the earth's surface. The discontinuity gives rise to a critical angle θ_c for rays incident from the more dense medium. We define

$$\theta_c = \arccos \frac{n_2}{n_1} \qquad (1)$$

where n_1 is the refractive index of the more dense medium (=1 in this case) and n_2 is the refractive index of the ionized medium.

Classical geometric optics predicts that rays incident at less than θ_c are totally internally reflected while rays incident at greater than θ_c are refracted according to Snell's and Fresnel's Laws. Since the electron density varies with height, then the critical angle is also height dependent and varies along the magnetic flux line which contains the discontinuity.

However, in this case because of the curvature of the magnetic field line we must extend the concepts of geometric optics to include the phenomenon of electromagnetic tunnelling. We discuss this in detail in subsequent sections.

At heights below 100 km the discontinuity is considered to be so small as to be negligible.

2.2 The Ray approximations

2.2.1 Ray concepts

An electromagnetic wave propagating in free space has a well defined direction of propagation specified by wave vector $\underset{\sim}{k}$ normal to the electric and magnetic field vectors, $\underset{\sim}{E}$ and $\underset{\sim}{H}$ respectively. The vectors $\underset{\sim}{E}$, $\underset{\sim}{H}$ and $\underset{\sim}{k}$ form a right-handed triad. In a uniform homogeneous medium, no difficulty exists in the specification of the direction of the wave and the concept of a ray is easily managed. A ray indicates the direction of the local plane wave vector $\underset{\sim}{k}$, which is also the direction of power propagation. Maxwell's equations are exactly satisfied and the direction of the wave is simply the direction of a ray.

In an inhomogeneous medium, where the electromagnetic fields are not in general specified by a single plane wave, the direction of a ray is no longer so simply identified and it is necessary to specify it asymptotically as the short wavelength ($\lambda \to 0$) approximation for the local plane wave direction. It is used to indicate the direction of $\underset{\sim}{k}$ and the magnitude, given by the relation

$$|\underset{\sim}{k}| = k = \frac{2\pi n}{\lambda}, \tag{2}$$

is taken to the limit $k \to \infty$. λ is the wavelength of light in vacuum. The ray path is then always defined by the eikonal equation,

$$\frac{d}{ds}\left(n \frac{d\underset{\sim}{R}}{ds}\right) = \underset{\sim}{\nabla} n \tag{3}$$

where s is the distance measured along the path and $\underset{\sim}{R}$ is the position vector for a point on the ray path. n is the refractive index of the medium at the point under consideration and $d\underset{\sim}{R}/ds$ is interpreted physically as a unit vector tangent to the ray path. This is the asymptotic theory known as geometric optics. The ray direction defined in the short wavelength approximation is specified everywhere including caustics and points of reflection.

Indiscriminate use of geometric optics leads to strange contradictions. It predicts the field intensity at a focus or caustic to be infinite which is obviously ridiculous. The field distribution near caustics is not properly calculated using geometric optics and in order to allow the advantages of the simplicity of geometric optics to be exploited everywhere we aim to extend geometric optics to accommodate these effects. A similar approach has already been used by Keller(ref.9) in the Geometric Theory of Diffraction which has proved highly successful.

2.2.2 Ray tube concepts

Consider the situation shown in figure 2 where two rays are drawn through adjacent points on a wavefront within (a) a graded index and (b) a step index dielectric waveguide forming a characteristic flux tube as shown in each case. The flux or ray tube can be traced as shown through an optical medium by tracing each of the rays individually.

The region of depleted ionization we can regard as being the core of a dielectric waveguide while the region above it is exterior to the guide and has commonly been referred to as the cladding. When the core is non absorbing, power in the ray tube travels parallel to the ray direction and can only be lost to the cladding at reflections from the core cladding interface or at caustics where the asymptotic description of geometric optics is inadequate.

2.2.3 A model for attenuation

The definition of a ray allows us to associate with a ray power travelling in the same direction. Strictly speaking, the terminology should refer to either a small ray tube or flux tube but it is simpler, physically appealing and unambiguous to merely refer to it as the power of the ray.

In a guiding structure the local plane wave fields of a family of rays, all with the same ray invariants and following similar ray paths, is the geometric optics equivalent of a mode(ref.7). In order to develop a ray model for attenuation it is convenient to introduce the concept of a ray transmission coefficient. If the refractive index of the core is n_1 and of the surrounding medium is n_2 with $n_2 < n_1$, then the ray suffers reflections within the core of the guide losing a fraction of its power at each reflection. An equivalent situation exists for graded media, where a ray loses power each time it touches the outer caustic or turning point along the ray path in the core.

The ray power transmission coefficient T is defined as

$$T = \frac{\text{Power lost from the incident ray}}{\text{Power in the incident ray}} \tag{4}$$

The value of T represents the fraction of power lost at each reflection and for an asymmetrical guide, such as we have here, it can vary from one reflection to the next. This definition is equivalent to the definition of the classical ray transmission coefficients of Fresnel.

The model for ray attenuation is formulated as follows. Consider the situation where a ray carrying initial power P_o at $z = 0$ undergoes a fractional loss T_1 at the first reflection, then after this reflection there will be an amount of power P_1 left travelling along the ray, where

$$P_1 = P_o(1 - T_1) \tag{5}$$

After a second reflection we have power P_2 left in the ray,

$$P_2 = P_o(1 - T_1)\ (1 - T_2) \tag{6}$$

where T_2 denotes the loss at the second reflection. After n reflections the remaining power is

$$P_n = P_o \prod_{i=1}^{n} (1 - T_i) \tag{7}$$

If the distance to the first reflection is z_{p1} and the distance between the i - 1'th reflection and the i'th reflection is z_{pi} then the distance travelled along the guide by the ray to the n'th reflection is

$$z_n = \sum_{i=1}^{n} z_{pi} \tag{8}$$

It is convenient to express the power variation along the guide in the form of

$$P(z) = P(o) \exp(-\gamma_R z) \tag{9}$$

Recasting (9) as

$$-\gamma_R z = \ln \frac{P(z)}{P_o} \tag{10}$$

and substituting P_n for $P(z)$ and z_n for z gives

$$-\gamma_R \sum_{i=1}^{n} z_{p_i} = \sum_{i=1}^{n} \ln(1 - T_i) \tag{11}$$

or

$$\gamma_R = - \frac{\sum_{i=1}^{n} \ln(1 - T_i)}{\sum_{i=1}^{n} z_{p_i}} \tag{12}$$

Only when $T_i \ll 1$ does (12) reduce to the simple form

$$\gamma_R = \frac{\sum_{i=1}^{n} T_i}{\sum_{i=1}^{n} z_{pi}} \tag{13}$$

The waveguide loss between the transmitter A and the receiver B is therefore

$$P(z) = P(o)\exp\left\{ - \sum_{i=1}^{n} \ln(1 - T_i) \right\} \qquad (14)$$

if we chose to ignore small effects such as the Goos-Hänchen shift(ref.10).

This then becomes a powerful method for solving large numbers of dielectric waveguide problems.

2.3 A model for received power

So far we have examined some simple two-dimensional models needed for a geometric optics based solution for the waveguiding problem. We first of all need to extend these concepts to three dimensions before we can calculate the received power at B.

The power received by an antenna P_R is given by

$$P_R = \text{power density (D) x effective area (A)} \qquad (15)$$

where the aerial capture area is

$$A = G_R\left(\frac{\lambda^2}{4\pi}\right), \qquad (16)$$

G_R is the gain of the receiving antenna and λ is the wavelength.

The power density within a flux tube is

$$D = \frac{\text{fraction of transmitted power in flux tube}}{\text{area of tube}} \qquad (17)$$

For a small flux tube the fraction of the total solid angle subtended is

$$\frac{d\theta\, d\phi}{4\pi}$$

and substituting this in (17) and using (15) and (16) we get the conventional free space formula

$$P_R = \frac{P_o . G_t . G_R}{R^2} \left(\frac{\lambda}{4\pi}\right)^2$$

Where guidance is involved then the cross sectional area of the tube is $\ell R d\phi$ and

$$P_R = \frac{P_o . d\theta/4\pi}{R.\ell} . \frac{\lambda^2}{4\pi} . G_t . G_R \qquad (18)$$

where l is the width of the flux tube and $d\theta$ is the angular width of the tube in the dimension in which guidance occurs as illustrated in figure 3. It is important to note that this implies $\frac{1}{R}$ dependence in the orthogonal dimension, ie no guidance in the $d\phi$ direction. If there is curvature in the plane normal to the xy plane defined on figure 10 then additional focussing would be achieved. That avenue has not yet been investigated. As far as the ray tracing procedure is involved we see that it is necessary only to calculate ℓ. If guidance also occurred in the orthogonal direction then it would also be necessary to calculate the depth of the flux tube as well.

If power is lost from the flux tube by either absorption or tunnelling(ref.11) then the power received must be attenuated according to equation (14) since it is the total power only which remains constant not just the propagated power. This extension of geometric optics enables us to take account of curvature losses in the same way as Keller(ref.9) takes account of diffraction terms.

We therefore have a method of calculating the received power within each particular flux tube enhanced by the gains of the receiver and transmitter antennae. As the number of flux tubes increases the power density approaches its limiting value.

If the transmitter situated at A has the antenna polar diagram specified in Appendix IV then the power transmitted into the ionosphere can be described in terms of ray concepts, with the power associated with each ray being determined from the antenna polar diagram. In what follows the gains of the antennas will be normalised to a standard dipole ($G_t=G_R=1.6$) but still including the effects of earth reflection at both A and B according to Appendix IV.

It is straightforward to calculate the points of intersection of each ray with the magnetic field line and its locus in between until it intersects the surface of the earth in the opposite hemisphere. The geometry for the intersection of a ray and the magnetic field line is written down in Appendix V.

At each point of intersection the ray transmission coefficient T is calculated using the Generalized Fresnel's Law(ref.11) for reflection from a curved dielectric interface. This law incorporates the geometric optics extensions needed to account for tunnelling transmission. Then summing over all flux tubes originating from the transmitter, contours of the received power for points near B can be derived.

3. RESULTS

The equations described in the previous section were programmed onto a high-speed digital computer to calculate the power received at B from a transmitter at A. The power was normalised with respect to 1 kW of transmitter power and standard dipoles at each end of a circuit between Darwin and Yamagawa whose coordinates are listed in Table 1 below.

The powers received in dB with respect to one milliwatt are plotted in figures 4 to 8 against range from the geomagnetic equator for wavelengths of λ = 3.0, 4.0, 4.5, 5.0 and 6.0 m. The maximum height of the magnetic field line coincident with the dielectric discontinuity is taken to be 600 km and the critical frequency which is determined by the ionization density is taken to correspond with the predictions of the Ionospheric Prediction Service (IPS) Series U publications for March to April 1970. The position B corresponds to the range of 2170 km from the equator.

Experimental results for this circuit have been analysed by Kuriki et al (refs.12,13) and plotted against frequency. Their results were averaged over two periods corresponding to the autumnal and vernal equinoxes for a period of several months during 1970. We estimate the average critical frequency for March to April as f_c = 10.2 Mc/s and for September to October as f_c = 10.8 Mc/s. The results show an absolute agreement to within 6 dB with the results of our idealised computer model over the whole range of frequencies 50 to 100 Mc/s. The comparison is shown plotted in figure 9.

Preliminary investigations show that the maximum height of the field line required to give these results is about 50% higher than the height of the peak in the ionization density. If it was lower then the magnitude of the dielectric discontinuity on the walls would be insufficient to maintain guidance while if it was higher then the ionization at the top of the field line would be insufficient.

As yet the reason for the bulge in the experimentally observed results near 88 MHz has remained obscure but this bulge was not observed in the results of Bowen et al(ref.14) or Nielson(ref.1) in their results. However, the variation of received power with frequency is not linear as proposed by Kuriki et al(ref.13) even though over a limited range of frequencies it may appear to be. He used a theory based on scattering from ionospheric irregularities but needed to make questionable assumptions regarding the nature of scattering from these irregularities and their frequency of occurrence. His scattering theory produced the straight line with f^{-10} dependence superimposed on figure 9.

In contrast the calculations used in this model attribute the power to guidance rather than scattering and rely merely on the existence of field aligned irregularities that are likely to be associated with rising plasma bubbles. Discrepancies between observed and calculated results could easily be due to imperfections in the shape or continuity of the elliptical surface assumed in this model. Alternatively, if the ionization within the bubble was not totally depleted then a slightly smaller critical angle would be associated with points on the ellipse and this would reduce the received power.

Changes in the critical frequency of 6% observed between the autumnal and vernal equinoxes produces only a ½ dB change in the received power for the Darwin/ Yamagawa circuit at λ = 6 m using this geometry rather than the 3 dB observed experimentally.

Since the results of this initial investigation are so close to the experimental results further analysis appears to be warranted. In a subsequent study we will perturb all the parameters associated with this model to determine their allowable range and to seek an experimental method of confirming their behaviour.

4. CONCLUSIONS

A simple model for the received power on a transequatorial circuit described by figure 1 has been proposed which may explain night-time radio wave propagation in the ionosphere. The mechanism has been ascribed to guidance along field aligned irregularities associated with rising plasma bubbles in the ionosphere. Good agreement has been demonstrated between experimental results obtained on a circuit between Darwin and Yamagawa and theoretical results for an ideally formed guiding irregularity.

Further investigation is required to optimise the model, to determine an experimental technique of validating it and to evaluate the effect of imperfections in the guiding surface.

REFERENCES

No.	Author	Title
1	Nielson, D.L.	"Long range VHF propagation across the geomagnetic equator". Stanford Res. Ins. Report, March 1969
2	Booker, H.G. and Ferguson, J.A.	"A theoretical model for equatorial ionospheric spread F echoes in the HF and VHF bands". J. Atmos. Terr. Phys., Vol. 40, p 803, January 1978
3	Woodman, R.F. and La Hoz, C.	"Radar observations of F region equatorial irregularities". J. Geophys. Res., Vol. 81, p 5447, November 1976
4	Dyson, P.L. and Benson, R.F.	"Topside sounder observations of equatorial bubbles". J. Geophys. Res., Vol. 5, p 795, September 1978
5	Heron, M.L. and McNamara, L.F.	"Transequatorial VHF propagation through equatorial plasma bubbles". Radio Sci. Vol. 14, p 897, Sept-Oct 1979
6	McClure, J.P. et al	"Plasma bubbles and irregularities in the equatorial ionosphere". J. Geophys. Res., Vol. 82, p 2650, July 1977
7	Love, J.D. et al	"Rays and modes in step index multimode elliptical fibres". Micro. Opt. Accous., Vol. 3, p 231, November 1979
8	Winkler, C.	"Theory and application of ray transmission coefficients in multimode optical fibres". Ph.D. thesis, Aust. Nat. Univ. 1978
9	Keller, J.B.	"Geometric theory of diffraction". J. Opt. Soc. Am., Vol. 52, p 116, July 1962
10	Love, J.D. and Winkler, C.	"Goos-Hänchen shift for leaky rays on step index waveguides". Electron. Letts., Vol. 14, p 379, June 1978
11	Snyder, A.W. and Love, J.D.	"Reflection at a curved dielectric interface - electromagnetic tunnelling". IEEE Trans. MTT-23, p 134, January 1975
12	Kuriki, I. et al	"Propagational mode deduced from signal strengths in the VHF band on the trans-equatorial path". J. Radio Res. Labs., Vol 19, p 175, June 1972

No.	Author	Title
13	Kuriki, I. et al	"Some characteristics of VHF propagation between Australia Japan". 5th International Symposium of Equatorial Aeronomy, Townsville, August 1976
14	Bowen, E.D. et al	"VHF characteristics of the transequatorial ionosphere". J. Geophys. Res., Vol. 73, p 2469, April 1978
15	Winch, R.P.	Electricity and Magnetism, Prentice Hall, 1959, p 350
16	Budden, K.G.	Radio Waves in the ionosphere, Cambridge University Press, 1961

NOTATION

b	intercept of ray with y axis
c	variable defined in Appendix V
f_c	critical frequency
f_N	plasma frequency
h	maximum height of field line chosen
$\underset{\sim}{k}$	wavenumber
$k_{y_1}, k_{y_2}, k_{y_3}, k_{y_4}$	component of wave vector $\lvert \underset{\sim}{k} \rvert$
m	ray slope
m_1	incident ray slope
m_2	slope of ellipse at point of reflection
m_3	reflected ray slope
n_1, n_2	refractive indices
r	polar coordinate for point on field line
A	minor semi axis of ellipse
B	major semi axis of ellipse
H	ionospheric scale height
H_1	antenna height
N	electron density
R	radius of earth
T	ray transmission coefficient
T_F	Fresnel coefficient
α	coefficient of α Chapman layer
ϵ	dielectric permittivity
λ	wavelength of source
θ_c	critical angle
θ_i	angle of incidence
ρ_c	radius of curvature of ellipse at point of reflection

ϕ	phase path difference
Δ	ray direction from transmitter
Φ	variable defined in Appendix IV

APPENDIX I

STRUCTURE OF THE EQUATORIAL FIELD

The equation of a metnetic field line from a point magnetic dipole located at the centre of the earth is given by the equation(ref.15)

$$\frac{r}{\cos^2\theta} = \text{constant} \tag{I.1}$$

where r, θ are the polar coordinates of a point on the field line as shown in figure 10. The intersection of a field line, which passes through a maximum height h at the geomagnetic equator (G), with the surface of the earth (radius R) occurs where latitude θ is given by

$$\theta = \pm\arccos\sqrt{\frac{R}{R+h}} \tag{I.2}$$

In the local plane cartesian coordinates Oxy position of the intersection is at $(R\sin\theta, R\cos\theta - R/2)$.

If the discontinuity is assumed to begin at conjugate points on opposite sides of the equator S, S' at a height of 100 km then in local cartesians Oxy the points S, S' using equation (I.2) are at $(R + 100)\sin\theta'$, $(R + 100)\cos\theta'$, $-R/2$, where θ' is the latitude of intersection of the field line contour and the contour 100 km above the earth's surface. Fitting an ellipse to the points G, S, S' gives a best fit curve having the equation

$$\left\{\frac{x}{(R+100)\sin\theta'\sqrt{1-\left(\frac{(R+100)\cos\theta' - R/2}{(R+h)/2}\right)^2}}\right\}^2 + \left(\frac{y}{(R+h)/2}\right)^2 = 1 \tag{I.3}$$

In the region of the equator the error involved in assuming the equation of the field line to be equation (I.3) for h = 500 km is less than 1% compared to equation (I.1) over the whole of the curve above the ground.

APPENDIX II

MODEL FOR ELECTRON DENSITY

An appropriate electron density model is the Chapman model defined by ≒ Reference 16. The frequency f_N is defined in terms of the critical frequency f_c by

$$f_N^2 = f_c^2 \exp(\alpha(1 - z - e^{-z}))$$

where

$$z = \frac{h - h\ max}{H}$$

$$\alpha = 0.5 \text{ for an } \alpha \text{ Chapman layer}$$

h max is the height of the electron density peak.

A plot of height against ionization density for varying values of H with f_c = 12 MHz, h max ≒ 400 km appears as Figure 11. We choose H ≒ 60 km to give the distribution of Booker(ref.2).

The electron number density N is then given by the formula

$$N = 1.24 \times 10^{-8} f_N^2$$

APPENDIX III

CHANGE IN REFRACTIVE INDEX AT AN IRREGULARITY

The fractional change $\Delta\epsilon$ in the dielectric permittivity ϵ in an ionized medium is related to the change in ionization density ΔN by the relation

$$\left(\frac{\Delta\epsilon}{\epsilon}\right)^2 = \frac{1}{\pi^2} r_e^2 \lambda^4 \overline{(\Delta N)^2}$$

where r_e is the classical radius of the electron

$$(2.82 \times 10^{-15} \text{ m})$$

Strictly, λ should be the wavelength taking into account the ionization density N, but for VHF propagation in this model we will take λ to be the free space wavelength. At the irregularity therefore we will see a change in the magnitude of the refractive index discontinuity with height and a corresponding change in the critical angle θ_c where

$$\theta_c = \arccos \frac{n_1}{n_2}$$

where n_2, n_1 are the refractive indices on either side of the discontinuity.

In the case of a totally depleted plasma bubble rising in the ionosphere we put $n_1 = 1$.

If we arrange $\overline{\frac{\Delta N^2}{N^2}} = 1$ then n_2 is determined and hence θ_c.

APPENDIX IV

ANTENNA POLAR DIAGRAMS

The polar patterns characterising either a transmitting or receiving antenna at height H_1 above the ground are assumed to be identifical. The received field is given by the sum of the direct and reflected wave amplitudes as depicted in Figure 12. At low angles we can assume that the reflection coefficient of the surrounding earth is -1 and if the wave amplitude is A then the total amplitude received assuming unity antenna gain is

$$= A\sin wt - A\sin(wt + \phi) \qquad \text{(IV.1)}$$

where

$$\phi = \frac{4\pi H_1}{\lambda} \sin\Delta \qquad \text{(IV.2)}$$

λ = operating wavelength

and

Δ = angle of propagation.

This reduces to

$$A\{\sin wt(1 - \cos\phi) - \cos wt \sin\phi\}$$

$$= A' \sin(wt - \Phi)$$

where

$$\Phi = \tan^{-1}\left(\frac{\sin\phi}{1 - \cos\phi}\right) \qquad \text{(IV.3)}$$

The magnitude of the power from a transmitting antenna in direction Δ is then

$$A'^2 = A^2(2 - 2\cos\phi) \qquad \text{(IV.4)}$$

APPENDIX V

THE GEOMETRY OF REFLECTION FROM AN ELLIPTICAL SURFACE

Simple geometry as shown in figure 13 is used to determine the angles of incidence and reflection at a dielectric discontinuity. If the equation of the ellipse is

$$\frac{x^2}{A^2} + \frac{(y - Y)^2}{B^2} = 1$$

and of the incident ray is $y = mx + b$ where b is determined by the initial conditions then the point of intersection is given by the solution

$$x = \frac{-A^2 mc + AB\sqrt{B^2 - c^2 + A^2 m^2}}{(B^2 + A^2 m^2)}$$

where

$$c = b - Y$$

The slope of the ellipse at the point of intersection is m_2 given by

$$m_2 = \frac{-xB}{A\sqrt{A^2 - x^2}}$$

If the angle of incidence measured with respect to the reflecting surface is $\theta_i = \arctan m_2 - \arctan m_1$ and the slope of the reflected ray is m_3 then

$m_3 = \tan \theta_r$

and

$$m_3 = 2m_2 - m_1$$

TABLE 1. COORDINATES OF DARWIN AND YAMAGAWA

	GEOGRAPHIC COORDINATES	LATITUDE RELATIVE TO GEOMAGNETIC EQUATOR
DARWIN	130° 50' E, 12° 20' S	19° 32' S
YAMAGAWA	130° 37' 06" E, 30° 12' 05" N	23° 0' N

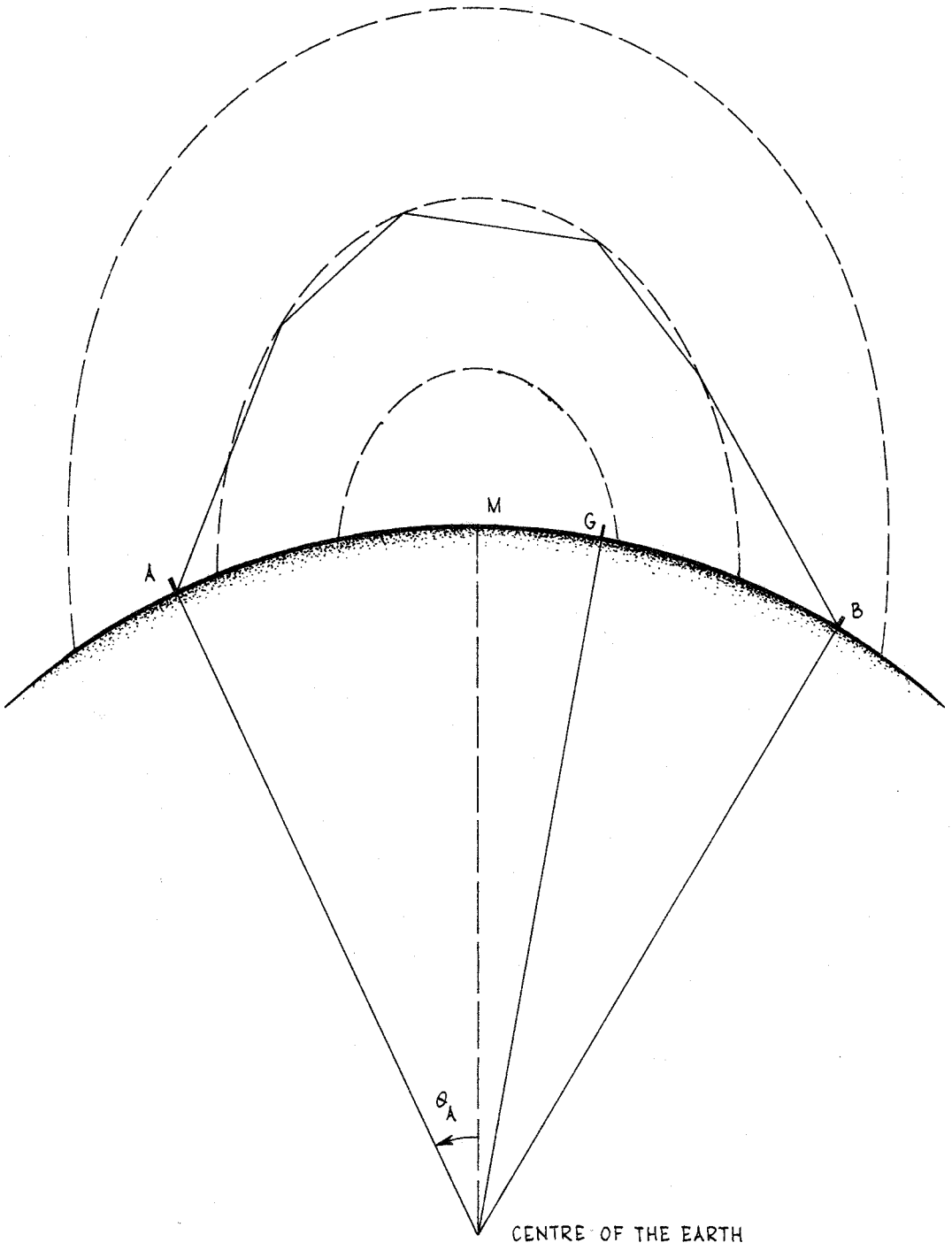

Figure 1. Power from a transmitter at A in one hemisphere is received at B on the opposite side of the geomagnetic equator

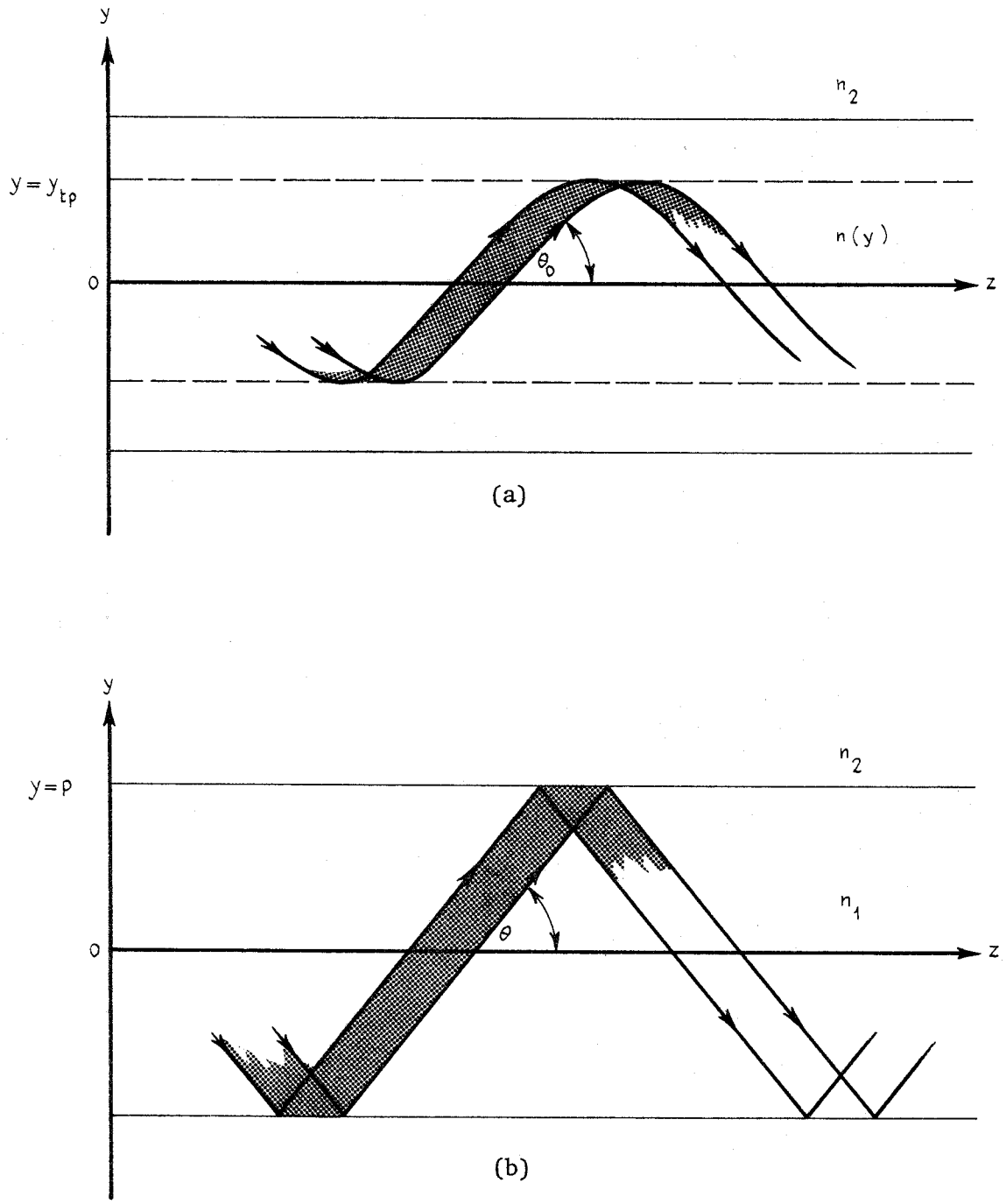

Figure 2. Sketch illustrating the formation of flux tubes from rays drawn through adjacent points on a wavefront in (a) a graded index and (b) a step index dielectric waveguide

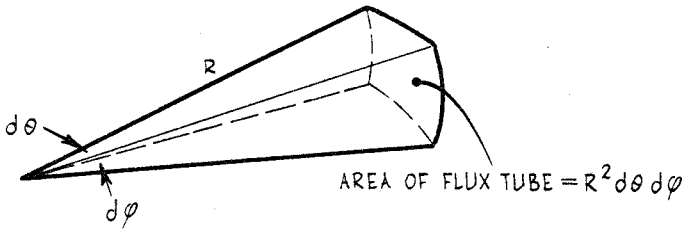

(a) Free space

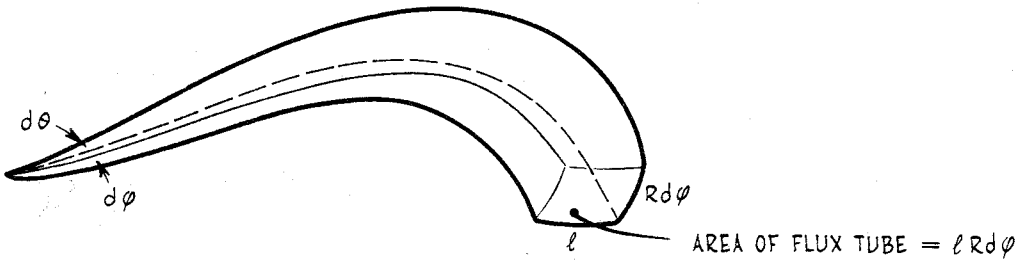

(b) Guided rays

Figure 3. Illustration of the construction of flux tubes in (a) free space, (b) where guidance is involved

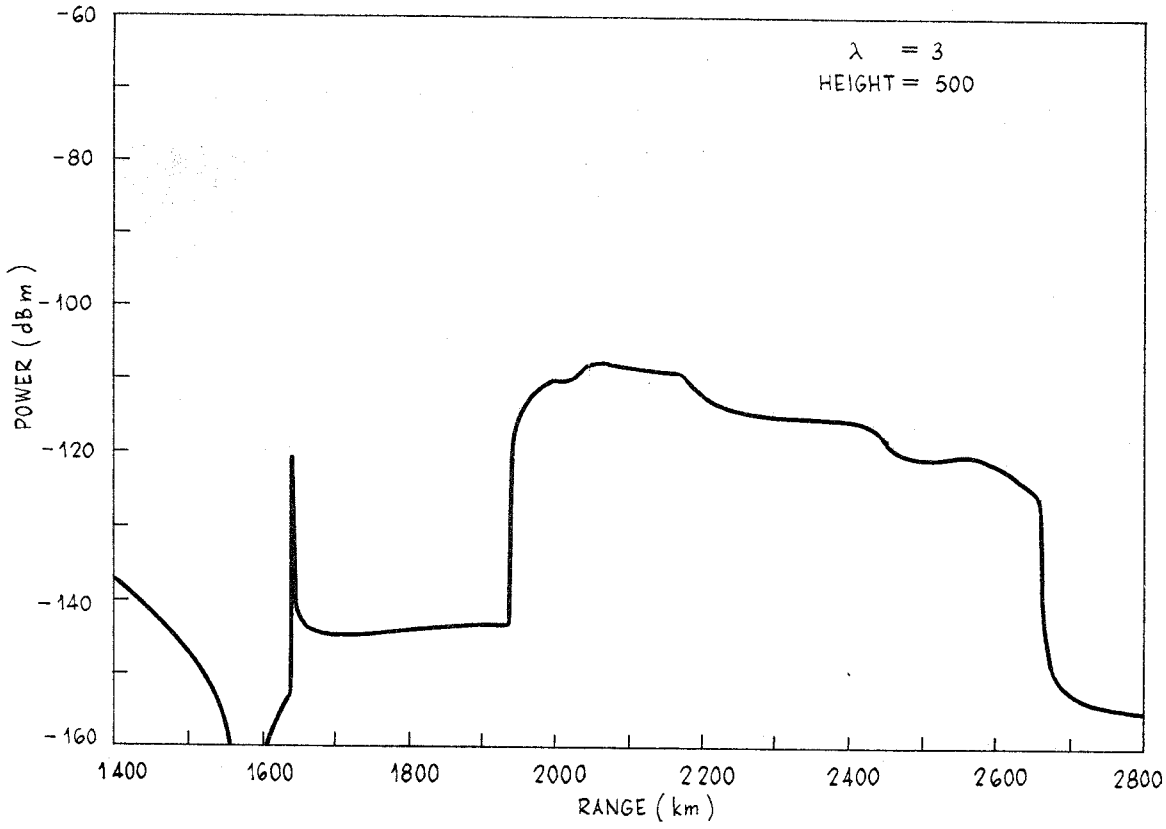

Figure 4. Plot of normalised received signal strength against distance from the equator for λ = 3.0 metres and h = 600 kilometres

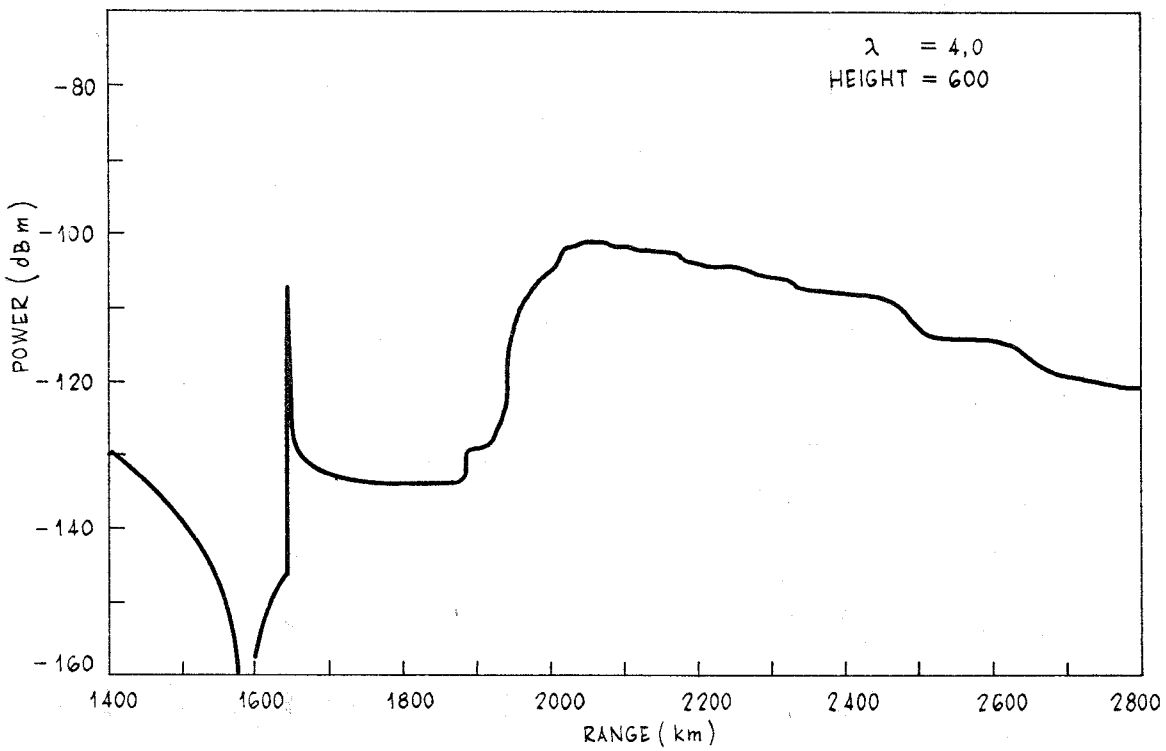

Figure 5. Plot of normalised received signal strength against distance from the equator for λ = 4.0 metres and h = 600 kilometres

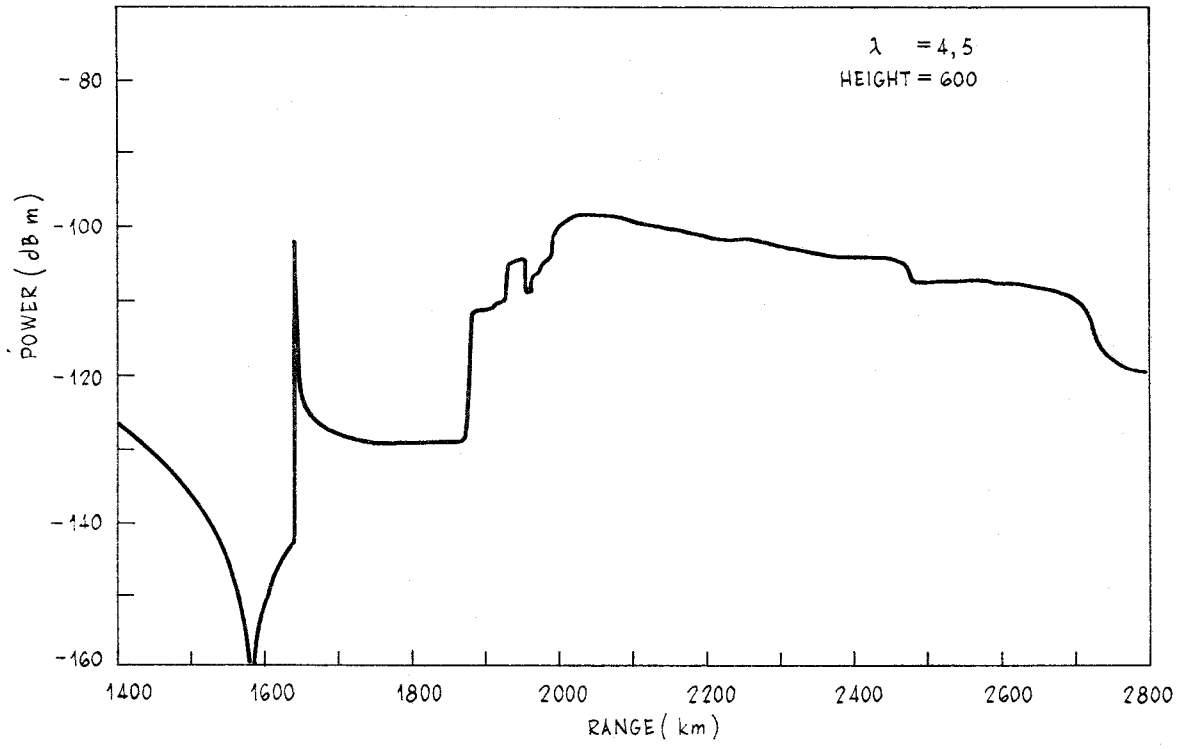

Figure 6. Plot of normalised received signal strength against distance from the equator for λ = 4.5 metres and h = 600 kilometres

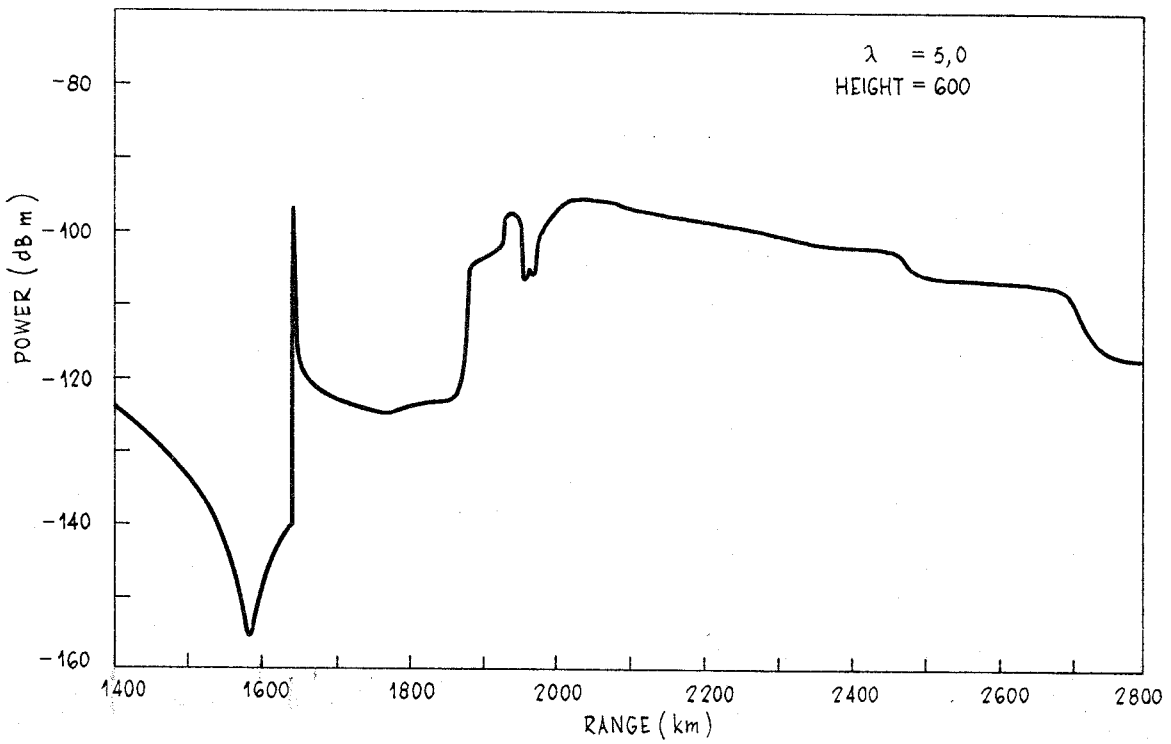

Figure 7. Plot of normalised received signal strength against distance from the equator for λ = 5.0 metres and h = 600 kilometres

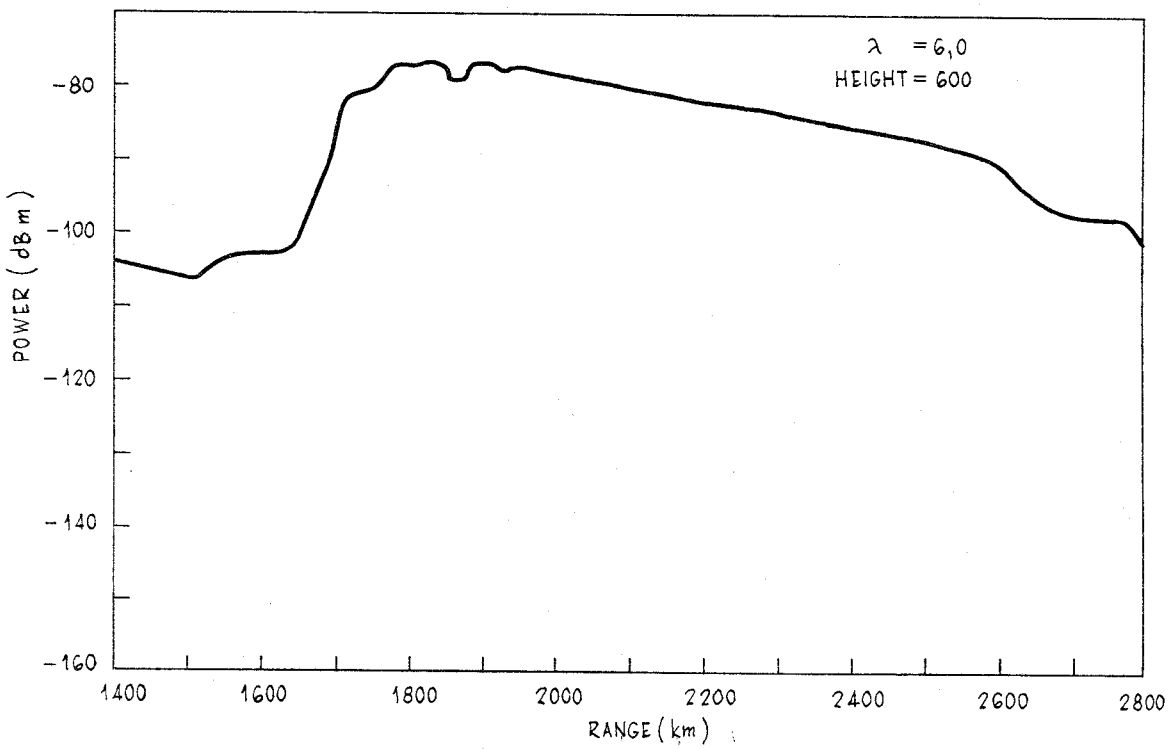

Figure 8. Plot of normalised received signal strength against distance from the equator for λ = 6.0 metres and h = 600 kilometres

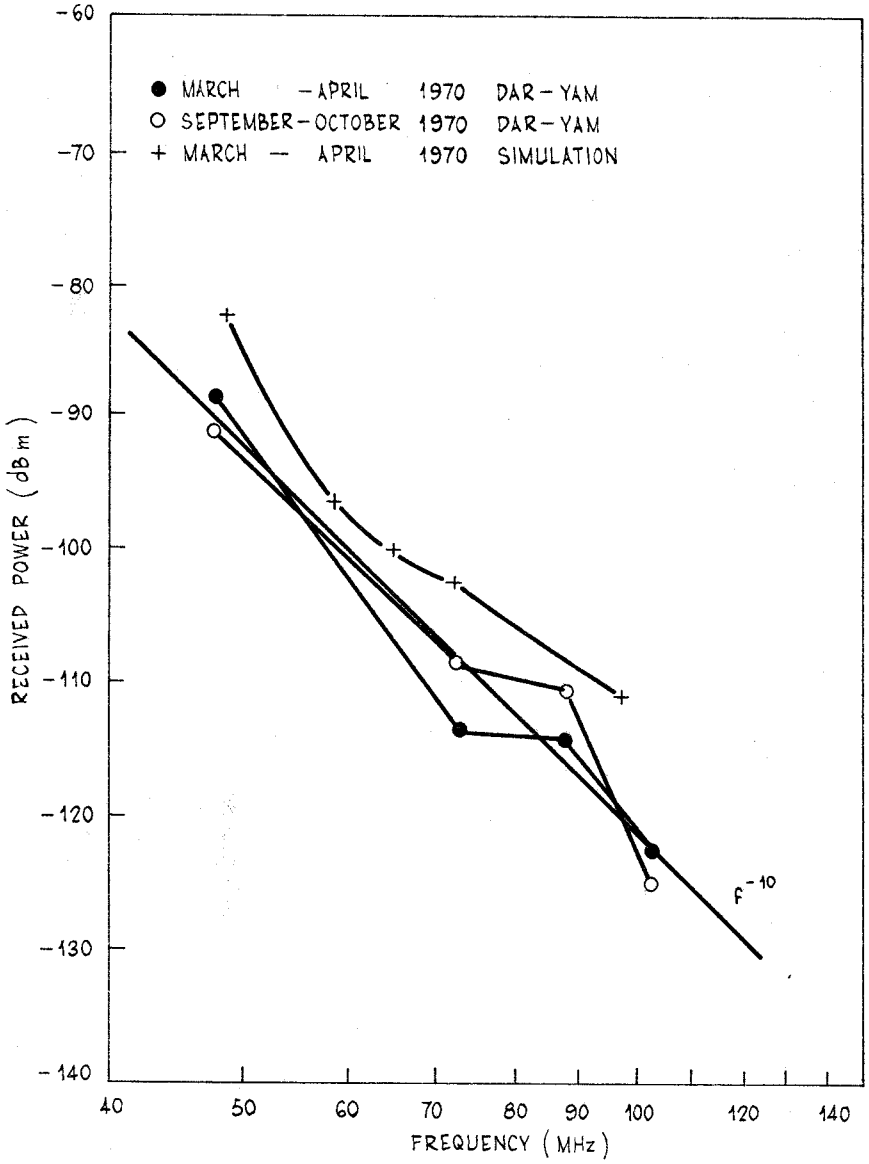

Figure 9. Plot of normalised received signal strength against frequency for both theoretical and experimental results as discussed in the text

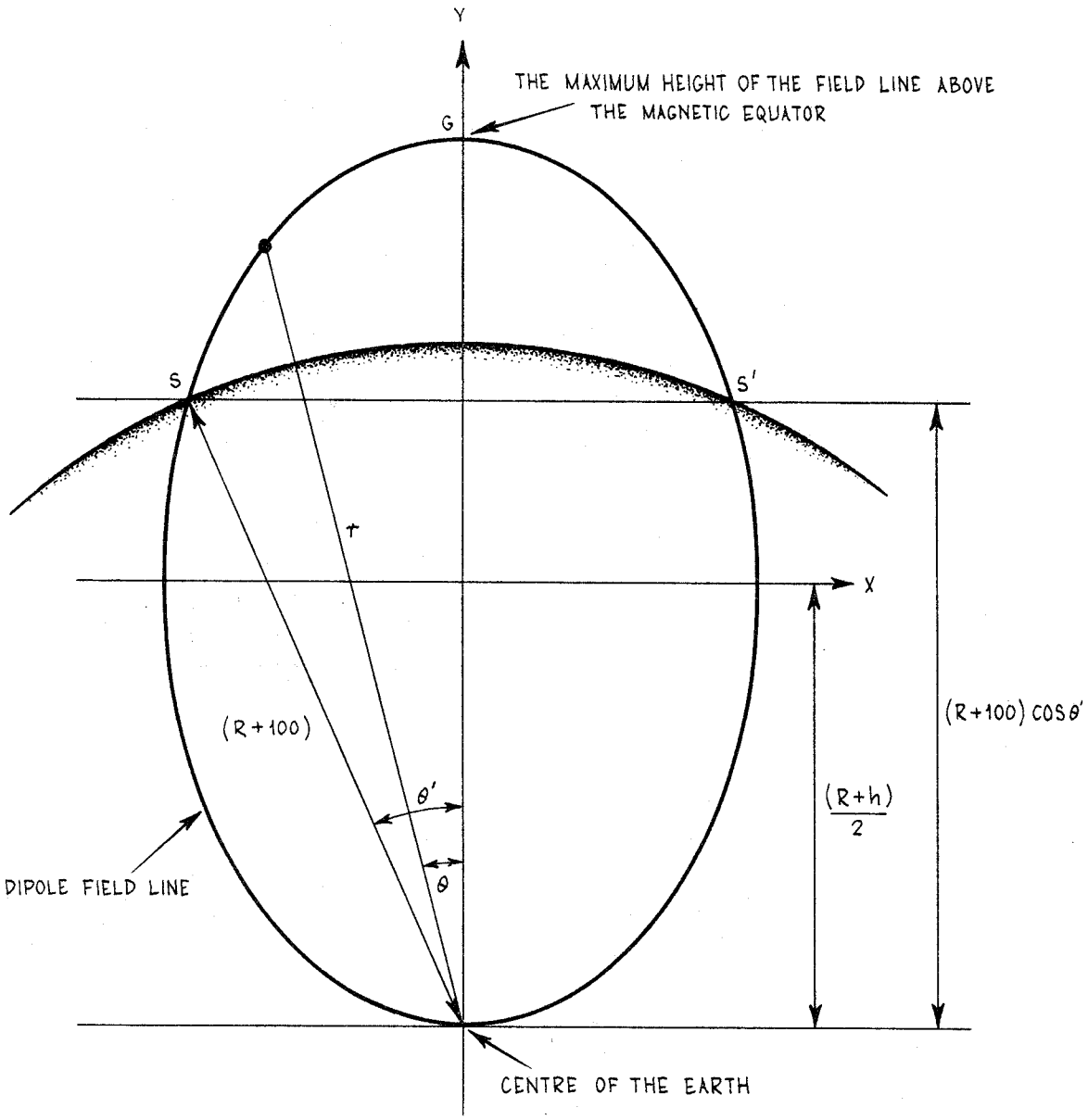

Figure 10. Geometry for fitting an ellipse to the dipole field line

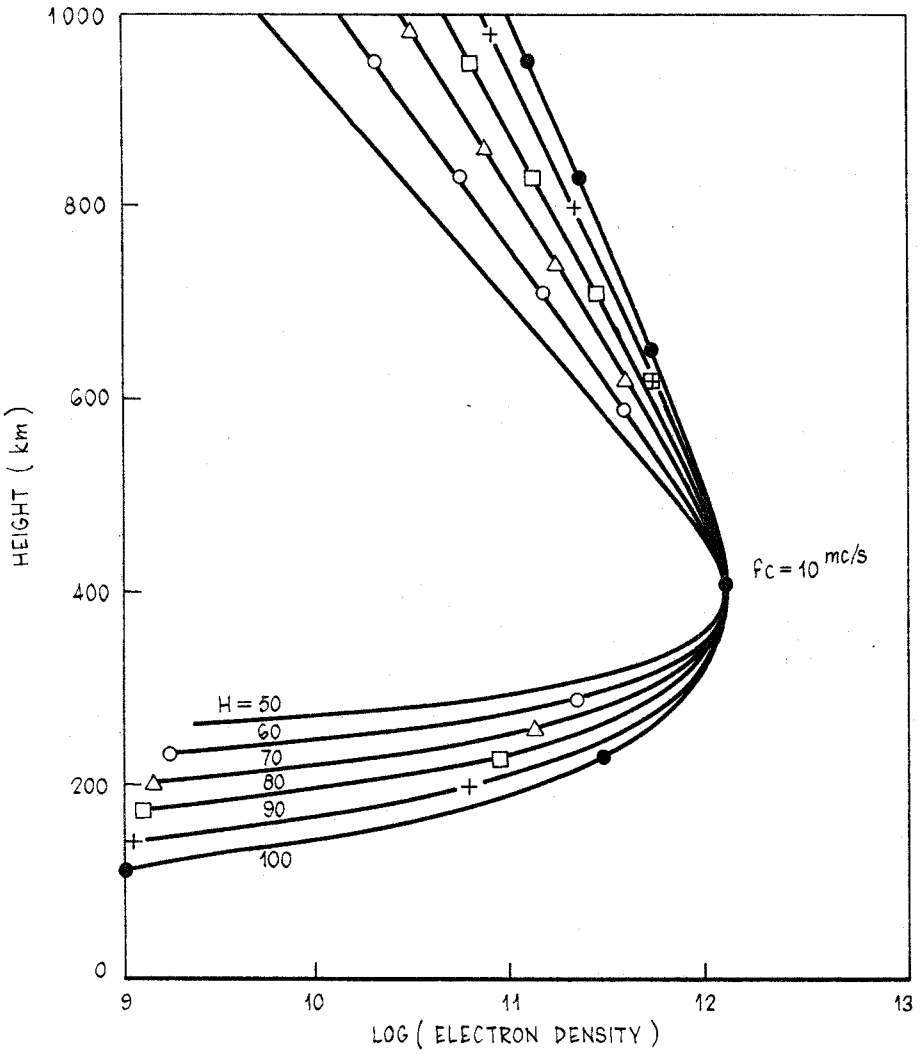

Figure 11. Plot showing relation between electron density and ionospheric height for an α Chapman layer using various values of scale height H

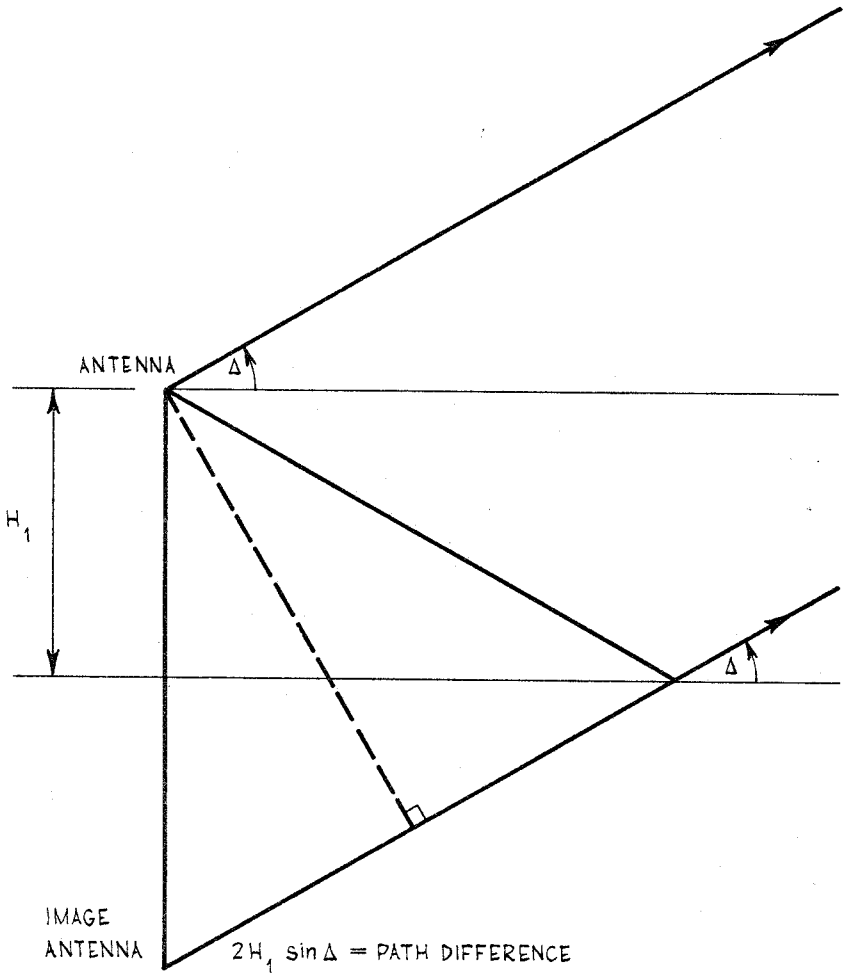

Figure 12. Geometry for Antenna Polar Diagram

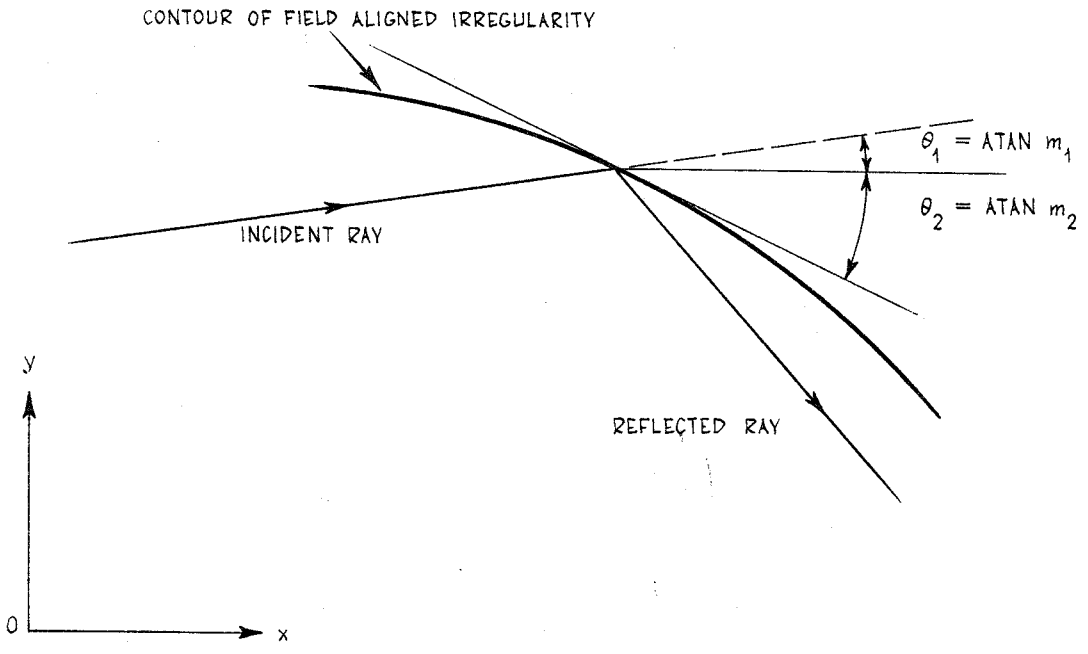

Figure 13. Geometry for reflection of a ray from an elliptic surface

DOCUMENT CONTROL DATA SHEET

Security classification of this page: UNCLASSIFIED

1 DOCUMENT NUMBERS

AR Number: AR-002-541

Report Number: ERL-0181-TR

Other Numbers:

2 SECURITY CLASSIFICATION

a. Complete Document: Unclassified

b. Title in Isolation: Unclassified

c. Summary in Isolation: Unclassified

3 TITLE

IONOSPHERIC TRANSEQUATORIAL RADIOWAVE GUIDANCE AT VHF

4 PERSONAL AUTHOR(S):

C. Winkler

5 DOCUMENT DATE:

January 1981

6 6.1 TOTAL NUMBER OF PAGES: 28

6.2 NUMBER OF REFERENCES: 16

7 7.1 CORPORATE AUTHOR(S):

Electronics Research Laboratory

7.2 DOCUMENT SERIES AND NUMBER

Electronics Research Laboratory 0181-TR

8 REFERENCE NUMBERS

a. Task: DST 74/023

b. Sponsoring Agency:

9 COST CODE:

174 844

10 IMPRINT (Publishing organisation)

Defence Research Centre Salisbury

11 COMPUTER PROGRAM(S) (Title(s) and language(s))

12 RELEASE LIMITATIONS (of the document):

Approved for public release

12.0	OVERSEAS	NO		P.R.	1	A		B		C		D		E	

Security classification of this page: UNCLASSIFIED

Security classification of this page: UNCLASSIFIED

13 ANNOUNCEMENT LIMITATIONS (of the information on these pages):

No limitation

14 DESCRIPTORS:

a. EJC Thesaurus Terms

Equatorial zone
Very high frequencies
Telecommunication
Radio waves
Computerized simulation
Ionospheric propagation
Mathematical models

b. Non-Thesaurus Terms

Transequatorial propagation
Geometric opties

15 COSATI CODES:

2014
1702

16 LIBRARY LOCATION CODES (for libraries listed in the distribution):

17 SUMMARY OR ABSTRACT:
(if this is security classified, the announcement of this report will be similarly classified)

The mechanism of reflection of radio waves at VHF from irregularities aligned with the earth's magnetic field in the equatorial region is examined in detail and a computer-based study of the resulting phenomenon is presented.

Security classification of this page: UNCLASSIFIED